



Drug-Resistant Epimutants Exhibit Organ-Specific Stability and Induction during Murine Infections Caused by the Human Fungal Pathogen *Mucor circinelloides*

Zanetta Chang,^a Joseph Heitman^a

^aDepartment of Molecular Genetics and Microbiology, Duke University Medical Center, Duke University, Durham, North Carolina, USA

ABSTRACT The environmentally ubiquitous fungus *Mucor circinelloides* is a primary cause of the emerging disease mucormycosis. *Mucor* infection is notable for causing high morbidity and mortality, especially in immunosuppressed patients, while being inherently resistant to the majority of clinically available antifungal drugs. A new, RNA interference (RNAi)-dependent, and reversible epigenetic mechanism of antifungal resistance—epimutation—was recently discovered in *M. circinelloides*. However, the effects of epimutation in a host-pathogen setting were unknown. We employed a systemic, intravenous murine model of *Mucor* infection to elucidate the potential impact of epimutation *in vivo*. Infection with an epimutant strain resistant to the antifungal agents FK506 and rapamycin revealed that the epimutant-induced drug resistance was stable *in vivo* in a variety of different organs and tissues. Reversion of the epimutant-induced drug resistance was observed to be more rapid in isolates from the brain than in isolates recovered from the liver, spleen, kidney, or lungs. Importantly, infection with a wild-type strain of *Mucor* led to increased rates of epimutation after strains were recovered from organs and exposed to FK506 stress *in vitro*. Once again, this effect was more pronounced in strains recovered from the brain than from other organs. In summary, we report the rapid induction and reversion of RNAi-dependent drug resistance after *in vivo* passage through a murine model, with pronounced impact in strains recovered from brain. Defining the role played by epimutation in drug resistance and infection advances our understanding of *Mucor* and other fungal pathogens and may have implications for antifungal therapy.

IMPORTANCE The emerging fungal pathogen *Mucor circinelloides* causes a severe infection, mucormycosis, which leads to considerable morbidity and mortality. Treatment of *Mucor* infection is challenging because *Mucor* is inherently resistant to nearly all clinical antifungal agents. An RNAi-dependent and reversible mechanism of antifungal resistance, epimutation, was recently reported for *Mucor*. Epimutation has not been studied *in vivo*, and it was unclear whether it would contribute to antifungal resistance observed clinically. We demonstrate that epimutation can both be induced and reverted after *in vivo* passage through a mouse; rates of both induction and reversion are higher after brain infection than after infection of other organs (liver, spleen, kidneys, or lungs). Elucidating the roles played by epimutation in drug resistance and infection will improve our understanding of *Mucor* and other fungal pathogens and may have implications for antifungal treatment.

KEYWORDS antifungal resistance, epigenetics, filamentous fungi

The fungal infection mucormycosis is caused by a group of related fungi, the most common of which are the genera *Rhizopus*, *Mucor*, and *Lichtheimia* (1). Mucormycosis encompasses a broad range of infections from cutaneous infections to invasive systemic disease, which can lead to rates of mortality greater than 90% (2, 3). The most

Citation Chang Z, Heitman J. 2019. Drug-resistant epimutants exhibit organ-specific stability and induction during murine infections caused by the human fungal pathogen *Mucor circinelloides*. mBio 10:e02579-19. <https://doi.org/10.1128/mBio.02579-19>.

Editor Antonio Di Pietro, Universidad de Córdoba

Copyright © 2019 Chang and Heitman. This is an open-access article distributed under the terms of the [Creative Commons Attribution 4.0 International license](https://creativecommons.org/licenses/by/4.0/).

Address correspondence to Joseph Heitman, heitm001@duke.edu.

This article is a direct contribution from Joseph Heitman, a Fellow of the American Academy of Microbiology, who arranged for and secured reviews by Anuradha Chowdhary, Vallabh Patel Chest Institute, University of Delhi, and Vincent Bruno, University of Maryland School of Medicine.

Received 30 September 2019

Accepted 8 October 2019

Published 5 November 2019

common manifestation of disease is rhino-orbito-cerebral mucormycosis, which is often seen in patients with predisposing factors such as immunosuppression or diabetes (4). Rates of mucormycosis are increasing worldwide, due in part to an increase in the prevalence of predisposing factors (4, 5). As the causative fungi are ubiquitous in the soil, outbreaks are often caused by exposure to environmental sources, ranging widely from environmental disasters such as tornadoes to contaminated hospital linen (6–8). Mucormycosis is highly drug resistant, and only three antifungal drugs are approved for treatment: amphotericin B, isavuconazole, and posaconazole (9, 10). Therefore, a better understanding of drug resistance in mucormycosis is necessary for improving the clinical outcomes of this emerging pathogen.

Among the Mucorales, the genus *Mucor* is unique in that it also serves as a genetic model. In addition to its pathogenic nature, it has been utilized to study aspects of fungal biology as diverse as biofuel production, RNA interference (RNAi), and light sensing (11–16). It also serves as a model for a novel mechanism of intrinsic, transient, and RNAi-dependent antifungal resistance known as epimutation. In epimutation, *Mucor* endogenous RNAi pathways are activated and induce silencing of various drug target genes, resulting in antifungal resistance (17, 18). The mechanism of epimutation requires the core RNAi pathway and competes with an alternative RNA degradation pathway in *Mucor* (19).

Here, we studied epimutation-based drug resistance with the antifungal drug FK506 (also known as tacrolimus). FK506 binds the target protein, FKBP12, which is encoded by the *fkbA* gene in *Mucor*. Mutation of FKBP12 or repression via RNAi-based silencing of *fkbA* leads to drug resistance (17, 20). The FKBP12-FK506 complex inhibits the calcium-calmodulin-activated protein phosphatase calcineurin, which is required for *Mucor* dimorphism and virulence (21, 22). Wild-type *Mucor* strains grow as yeast when exposed to FK506, whereas resistant strains are blocked in the dimorphic transition and grow exclusively as filamentous hyphae in the presence or absence of FK506 under aerobic conditions.

We report here the first observations of epimutation affecting antifungal resistance after *in vivo* passage through a systemic murine model of mucormycosis. Infection of mice with an epimutant strain resistant to FK506 revealed that epimutants are largely stable during the course of infection. However, when epimutants were observed to revert during *in vivo* infection, the reversion occurred most prominently in the brain compared to other organs analyzed. Interestingly, infection with a wild-type strain led to an increased induction of epimutant-based resistance when isolates were recovered from *in vivo* passage and then exposed to FK506 *in vitro*. Induction of resistance was also observed to be more frequent in fungal isolates recovered from the brain compared to other organs. These observations suggest that rapid reversion and induction of epimutation may facilitate fungal microbial responses to the transition between the environment and the host. Elucidating the mechanisms by which *Mucor* responds to stressful environmental conditions, including factors as diverse as vertebrate hosts and antifungal drug stress, advances our understanding of mucormycosis, fungal pathogens, and the mechanisms and pathways that lead to the development of antifungal drug resistance and its maintenance and loss.

RESULTS

Systemic intravenous infection of mice via retro-orbital inoculation. For the murine infections in this work, we developed a model of *Mucor* infection via the retro-orbital venous sinus (23). Intravenous infection of mice via tail vein injection of *Mucor* spores is an established model of systemic infection that results in high mortality (24). However, tail vein injections are technically challenging, which can influence reproducibility of experimental results. Therefore, we aimed to develop an alternative systemic infection model. The retro-orbital route of injection has been established to be safe and effective, and it has been shown to be equivalent to tail vein injection for systemic delivery of intravenous drugs; it has also previously been used to deliver larger moieties to systemic circulation, including monoclonal antibodies and tumor cells (25,

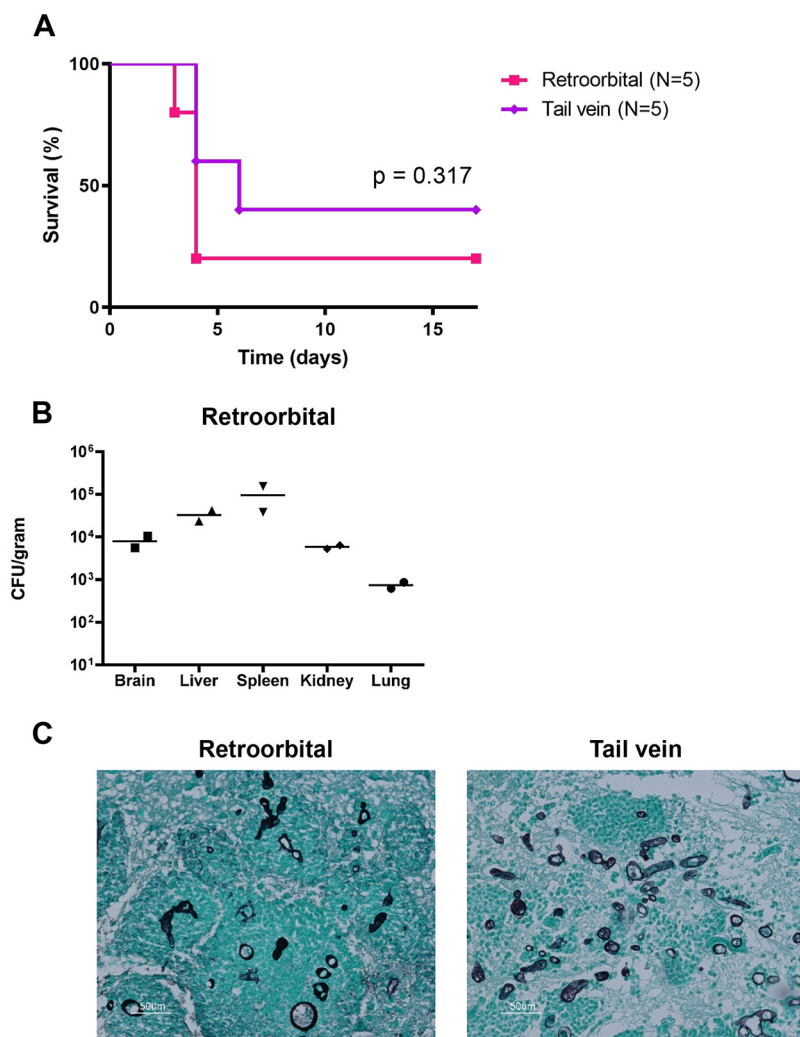


FIG 1 Retro-orbital and tail vein injections produce equivalent outcomes. BALB/c mice were infected with 1.25×10^6 spores of *M. circinelloides* f. *circinelloides* strain 1006PhL through either the retro-orbital or tail vein route. There were five mice in each group. (A) The two methods of infection produce equivalent mortality. (B) The retro-orbital method of infection produces equivalent homogenized fungal burdens in randomly sampled moribund mice ($N = 2$). (C) Histopathological analysis of brains from mice infected with spores by retro-orbital and tail vein injection, stained with GMS (Gomori methenamine-silver) reveals abundant fungal elements from both routes of infection.

26). In brief, mice are anesthetized with inhaled isoflurane, the area behind either eye is injected with fungal spores in saline solution, and the animal is removed from anesthesia and rapidly recovers over approximately 30 s.

To determine whether retro-orbital infection would produce the same course of disease as tail vein infection, we compared the two injection methods using groups of BALB/c mice (five mice per group). Spores of the 1006PhL strain of *Mucor circinelloides* f. *circinelloides* were injected into immunocompetent, wild-type mice by either the retro-orbital or tail vein method at a dose of 1.25×10^6 spores/100 μ l phosphate-buffered saline (PBS) per mouse. Despite longstanding experimental experience with the tail vein injection method, technical difficulties were experienced when injecting three of the five mice via tail vein, potentially due to the viscosity of the concentrated spore solution; no issues were noted with any animals in the study group while injecting retro-orbitally. All infections were allowed to progress until mice were euthanized at humane endpoints. No significant difference was noted between retro-orbital and tail vein groups with regard to survival time (Fig. 1A). Moribund fungal burden in five organs (brain, liver, spleen, kidney, and lung) was reproducible in two randomly

sampled mice from the retro-orbital group (Fig. 1B). Histopathologic analysis of animals by the Duke Research Animal Pathology Service revealed vascular, multifocal dissemination of fungal elements in organs after both retro-orbital and tail vein routes of infection (Fig. 1C).

Epimutants are largely stable and revert in an organ-specific fashion during murine infection. To examine the role epimutation might play in infection, strains were recovered after one *in vivo* passage through a mouse. Immunocompetent mice were infected retro-orbitally with either wild-type *Mucor* strain 1006PhL or the *fkba* epimutant strain SCV522. After 4 days, the moribund mice were euthanized with CO₂, and five organs (brain, liver, spleen, kidney, and lung) were dissected and homogenized. Organ homogenates were plated on nonselective yeast extract-peptone-dextrose (YPD) plus antibiotic (YPD + antibiotic) agar; plates were incubated at room temperature under hypoxic conditions, which drives *Mucor* growth into discrete yeast colonies instead of hyphae, to facilitate enumeration of CFU (27). In addition, the spores of strains SCV522 and 1006PhL that were used to infect the mice were also plated on nonselective YPD + antibiotic agar under the same hypoxic conditions. After 2 days, the resulting yeast colonies were removed from hypoxia and patched onto YPD and YPD plus FK506 (YPD + FK506) media to test for FK506 resistance. Patched plates were grown under standard room conditions, in which normoxic exposure would lead to the resumption of hyphal growth.

The plates were imaged after 16 h of growth, and FK506-resistant (hyphal) versus FK506-sensitive (yeast) colonies were counted. All colonies grew as hyphae on nonselective YPD under normoxic conditions, as expected. Among strains isolated from the mouse infected with *fkba* epimutant SCV522, it was noted that the epimutant strain was largely stable *in vivo*. Reversion to FK506 sensitivity was found more often in strains recovered from the brain compared to other organs (Fig. 2A). When quantified, more than half of the brain isolates had reverted to FK506 sensitivity, while reversion in the other organs was much more limited. For a control, we demonstrated that no reversion was observed in colonies derived from the spore stock of strain SCV522 that was used for the infection but that did not undergo any *in vivo* passage. In contrast to SCV522 passage, none of the isolates recovered from the wild-type 1006PhL-infected mouse were able to acquire FK506 resistance over the short time period of incubation regardless of the organ site (Fig. 2B). Quantification of FK506 resistance was performed with a target number of 150 patched colonies from each organ condition; fewer colonies were used if less than 150 colonies were recovered from the organ homogenate (see Table S1 in the supplemental material).

Representative sensitive and resistant isolates were selected for further analysis from the strains recovered from organs after SCV522 infection. Small RNA (sRNA) hybridization revealed that all resistant strains expressed sRNAs against the *fkba* gene, as would be expected if they had maintained their resistance through epimutation (Fig. 2C). Strains that had reverted to sensitivity, regardless of organ of origin, no longer expressed sRNAs against *fkba* (Fig. 2C).

This brain-specific tendency toward reversion is also seen in an alternative *Mucor* model in which the mice are immunosuppressed with cyclophosphamide 2 days prior to infection. In this model, the mice are euthanized after 2 days due to a more rapid course of infection; however, the brain-specific reversion of epimutation is maintained (see Fig. S1A and C in the supplemental material). Similarly, analysis of representative sensitive and resistant isolates from all organs revealed that the phenotypic loss of FK506 resistance was correlated with the cessation of sRNA expression against *fkba* (Fig. S1B). Infection with strain 1006PhL in this model also does not lead to the development of FK506 resistance from the recovered wild-type isolates.

***In vivo* passage causes development of *fkba* epimutants in an organ-specific fashion after prolonged FK506 exposure.** *In vivo* passage in mice without drug exposure does not lead to direct induction of epimutation-based FK506 resistance. However, passage through a murine host does lead to increased rates of epimutation if recovered strains are exposed to FK506 for longer periods of time.

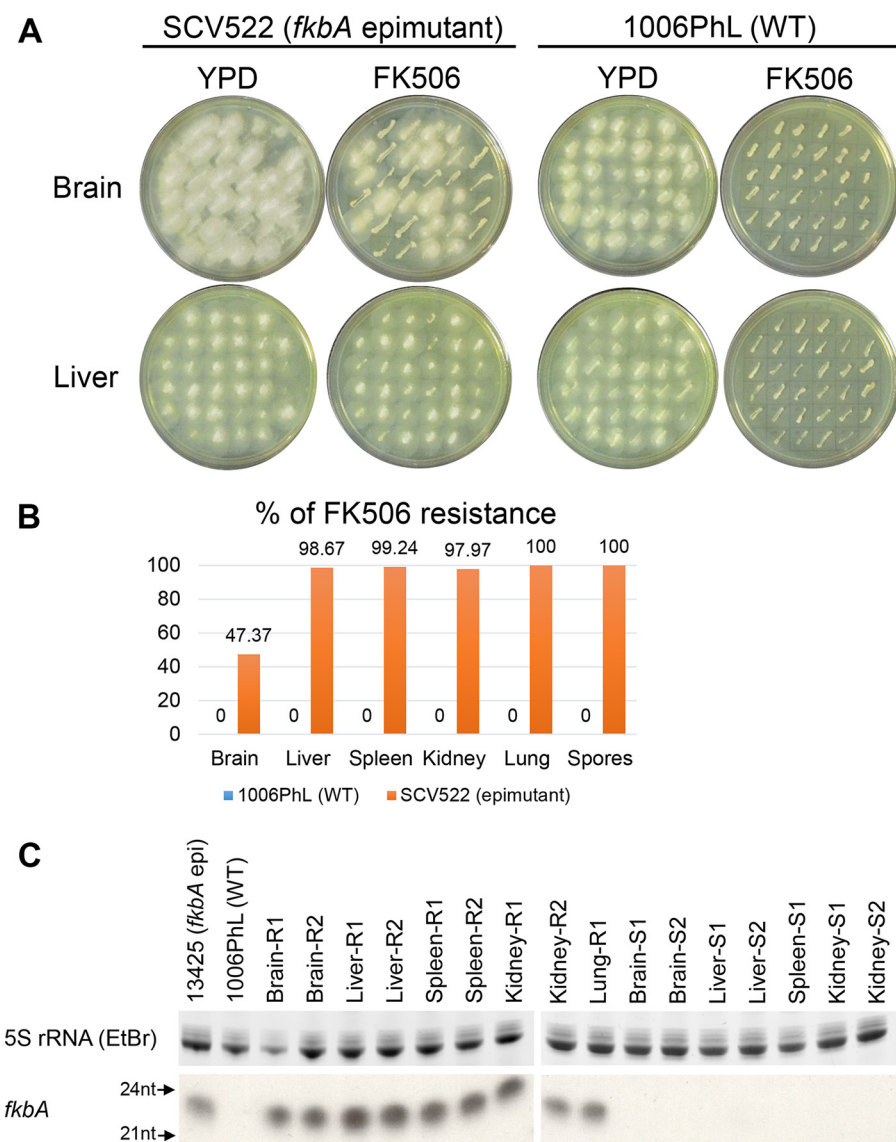


FIG 2 FK506 epimutants revert in an organ-specific manner after *in vivo* passage. *fkbA* epimutant and wild-type *M. circinelloides* f. *circinelloides* strains were recovered from multiple organs after *in vivo* infection/passage in one mouse each. Strains were recovered after the mouse was moribund, 4 days postinfection. Strain SCV522 is a *fkbA* epimutant. Strain 1006PhL is the wild-type (WT) strain. (A) Representative images of colonies recovered from the brains and livers of mice infected with either strain SCV522 or 1006PhL and patched onto YPD with and without FK506. All colonies patched on nonselective YPD medium grew as hyphae. FK506-sensitive strains patched on YPD + FK506 medium grew as smaller yeast colonies. Loss of FK506 resistance from the epimutant strain was observed in the brain, but not in the liver. (B) Quantification of the percentage of FK506 resistance by organ, after *in vivo* passage. There were 150 colonies per organ; however, fewer than 150 colonies were recovered from some organs (see Table S1 in the supplemental material). The Spores column shows SCV522 and 1006PhL spores plated without *in vivo* passage. FK506 resistance was below the limit of detection in all strains derived from wild-type 1006PhL infection. (C) sRNA hybridization of representative sensitive (S) and resistant (R) strains randomly selected from SCV522-infected mouse after passage. All resistant isolates continued to express sRNA against *fkbA*, whereas reverted, FK506-sensitive isolates did not. 5S rRNA was stained with ethidium bromide (EtBr) and served as the loading control. epi, epimutant; nt, nucleotides.

As in previous experiments, immunocompetent mice were retro-orbitally infected with wild-type 1006PhL spores and euthanized after 4 days when moribund. Organ homogenates from three mice were plated directly on YPD + antibiotics + FK506, as were spores from strain 1006PhL that did not undergo *in vivo* passage. Plates were incubated at room temperature with light for 5 days; during this growth period, sensitive yeast colonies arose, some of which transitioned to form resistant hyphal

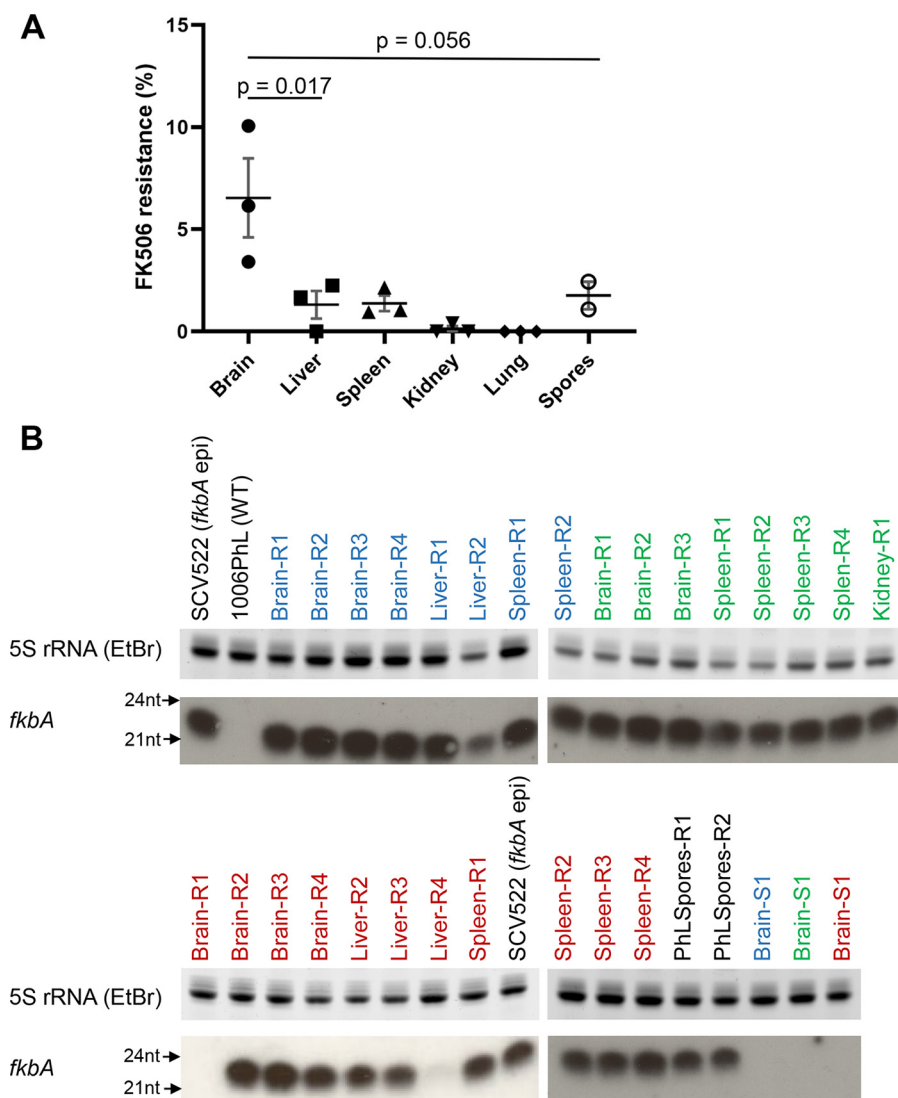


FIG 3 Organ-specific development of FK506 resistance after *in vivo* passage. Mice ($N = 3$) were infected with the wild-type 1006PhL strain; colonies were recovered on YPD + FK506 medium when mice were moribund, 4 days postinfection. Five days after recovery, resistant and sensitive colonies were counted. (A) Percentage of FK506 resistance by organ, showing higher rates of resistance in the brain. 1006PhL spores from strains without *in vivo* passage were plated and are shown in the graph. Significance was determined via one-way ANOVA ($P = 0.0035$) with *posthoc* Tukey's multiple-comparison test. (B) sRNA hybridization analysis against *fkbA* demonstrated the development of sRNA expression against *fkbA* in strains from all organs and spore conditions. SCV522 is the *fkbA* epimutant. 1006PhL is the wild-type strain. Strains isolated from each individual mouse are identified by the color of the label (blue, green, or red). Two of the 27 resistant (R) strains and all three of the sensitive (S) strains (one from each mouse) showed no evidence of sRNA expression against *fkbA*.

patches. Yeast and hyphal colonies from each organ were counted to calculate the percentage of FK506 resistance arising over time. Intriguingly, the most significant effect was once again seen with isolates from the brain (Fig. 3A). In this case, brain-derived isolates developed FK506 resistance at an average rate of 6.5%, higher than the rate observed in isolates from any other organ or from spores in isolates that did not undergo *in vivo* passage.

sRNA hybridization was performed to detect *fkbA* sRNA expression in representative FK506-sensitive and -resistant strains from each mouse (Fig. 3B). More than 90% (25 of 27) of the resistant strains expressed sRNA against *fkbA*, suggesting that epimutation is the predominant method by which resistance is gained after *in vivo* passage. The overall rate of FK506 resistance was much lower in strains derived from the liver, spleen,

kidney, or lung or in spores from strains that did not undergo *in vivo* passage; however, the predominant mechanism of resistance in these isolates was still based on sRNA. Sensitive strains isolated from the brain of each mouse did not express sRNA against *fkbA* (Fig. 3B).

DISCUSSION

The phenomenon of epimutation was recently characterized as a novel mechanism of RNAi-dependent drug resistance in *Mucor* (17–19). Here, we report the first analysis of the impact of epimutation during infection. We identified two contrasting epimutant-related phenomena that occur during a murine *in vivo* model of systemic mucormycosis. First, infection with an epimutant strain demonstrated that epimutation is maintained *in vivo* over the course of infection in multiple organs. Reversion of epimutation was markedly higher in the brains of mice than in other organs tested, at about 50%; this incomplete reversion may represent a bet-hedging strategy, enabling the fungus to respond to a range of environments. Second, *in vivo* passage of a wild-type strain of *Mucor* can lead to increased induction of epimutant-driven drug resistance, especially passage through the brain. This induction of epimutation does not appear to occur during the infection itself, but instead it arises several days after recovery of strains from organs under exposure to drug selection.

It is intriguing that growth in the brain appears to induce rapid changes in epigenetic states, including both reversion and induction of epimutation-driven FK506 resistance under different circumstances. One possibility is that there is simply more fungal replication in the brain, enabling more opportunities for stochastic toggling of epigenetic states. Clinically speaking, rhino-orbito-cerebral mucormycosis is the most common manifestation of disease, and this could reflect an aspect of the cerebral environment that makes the brain especially favorable for *Mucor* growth (2, 3). Histopathologic analysis of the systemic *Mucor* infections conducted in this study correlates with clinical evidence, as qualitatively more hyphal elements were visualized in the brain than in the other organs studied (Fig. 1C). Alternatively, instead of merely serving as a location for growth, the brain environment could provide a key, unidentified facet that induces epimutant switching. The rapid reversion effect was not replicated *in vitro* using commercially available media made from specific organs (tested using the bacterial medium brain heart infusion versus liver broth; see Fig. S2 in the supplemental material). We note that the presence or absence of cyclophosphamide immunosuppression in the mouse model did not alter the organ-specific nature of this reversion.

Another interesting observation in this study is that induction of epimutants in the brain was not immediate. Direct plating of wild-type strains recovered from the brain did not identify any strains with FK506 resistance; conversely, resistance arose only after several days of exposure to the antifungal once strains had been recovered from organs. This suggests that the brain environment is not directly inducing *fkbA* epimutants but perhaps is priming isolates in a manner which enables them to subsequently respond rapidly to stresses, including antifungal exposure. More than 90% of the resistant strains identified in this study were epimutants, which correlated with previously documented high rates of *fkbA* epimutant generation in the 1006PhL strain (17). Additional studies will need to be conducted to further examine induction of epimutation after *in vivo* exposure; it would be of interest to determine whether the rate of epimutation is increased in infected animals treated with clinical antifungals. Clinical courses of antifungal treatment for mucormycosis extend for weeks, much longer than the more limited time (a few days) required for development of resistance in this study (9). To date, there have been no reports of development of antifungal resistance during treatment for mucormycosis, but this phenomenon has been reported in other fungal infections (28, 29). In addition, we hypothesize that epimutation could mediate resistance to antifungal agents in clinical use for treatment of mucormycosis, including amphotericin B and isavuconazole, through silencing of the genes encoding the Erg3 and Erg6 enzymes. Drug resistance via loss of Erg3 or Erg6 requires further study in *Mucor* but has been demonstrated in a range of other pathogenic fungi (30–35).

Therefore, in sum, we hypothesize that epimutant-driven development of resistance over the extended course of clinical treatment represents a potential cause of treatment failure in mucormycosis and is worthy of further study.

This is the first example in which a stressful environmental condition—exposure to the host brain—has led to increased rates of epimutation in wild-type *Mucor*. Previously tested conditions which did not increase rates of epimutation included prior epimutation (induction of a second instance of epimutation from prior epimutant strains which reverted to wild type), antifungal drug exposure, cell wall stress, low nitrogen, low glucose, oxidative stress, and trisporic acid (mating conditions). The only method that increased the rate of epimutation was mutation of components of an alternative RNAi-based RNA degradation pathway (17). We have unsuccessfully attempted to replicate this brain-specific induction by testing various pH and hypoxia conditions (Z. Chang, unpublished data); additional study is required to elucidate the factor(s) that leads to this increased rate of resistance.

Given that *Mucor* is an environmentally ubiquitous fungus encountered on a global scale (36), it is also worthwhile to consider how non-host-pathogen interactions in the soil environment might affect traits such as epimutation. Epimutation is not limited to generating resistance to FK506 alone; it also functions to generate resistance to antifungals with entirely different mechanisms of action, such as the nucleotide analog 5-fluoroorotic acid (5-FOA) (18). Furthermore, antifungals, including FK506 and rapamycin, both of which bind to FKBP12, are known to be produced by members of the bacterial genus *Streptomyces*, which are found in soil (37, 38). We speculate that exposure to these and other antifungal compounds in the natural soil environment might lead to the development of clinically relevant epimutations similar to the *fkBA* epimutation, perhaps playing a role in the intrinsic resistance of *Mucor* to many antifungal drugs. These environmental epimutations could then be rapidly induced or reverted over the course of host infection, potentially serving as virulence factors that affect treatment and clinical outcomes.

Likewise, even during the course of a clinical infection, *Mucor* may not always be growing in a sterile organ environment such as the brain or liver. It is interesting to consider how fungal strains might interact with the polymicrobial components of the human microbiome at various body sites, whether during lung, skin, or gut infection. For example, instances of *Mucor* gastrointestinal illness from contaminated yogurt have been reported, and the etiologic strains were shown to alter the abundance of gut bacteria when fed to mice (39–41). An interesting future question might be whether the human microbiome is concurrently interacting with *Mucor* strains to influence the course of infection or development of drug resistance.

In summary, this study of epimutation revealed that epimutations affecting antifungal resistance can be both induced and reverted over the course of *in vivo* infection of *M. circinelloides*, with increased effects in the brain. Rapid switching of epigenetic states may enable adaptation to the very different environments in which *Mucor* can be found, from soil to invertebrate or vertebrate hosts. A better understanding of the mechanisms by which fungi can adapt to antifungal stress will improve our understanding of fungal biology and pathogenesis, while opening potential avenues for clinical treatment.

MATERIALS AND METHODS

Growth of strains. The *M. circinelloides* f. *circinelloides* strain 1006PhL served as the wild type for all studies. *fkBA* epimutant strain SCV522 was derived from strain 1006PhL in a prior study and recovered from -80°C laboratory freezer stocks (17). All strains were grown at room temperature (approximately 24°C) with normal daylight exposure. Strains were cultured on YPD agar (10 g/liter yeast extract, 20 g/liter peptone, 20 g/liter dextrose). The antifungal drug FK506 (Prograf, in a sterile formulation from Astellas Pharma) was sterilely added to YPD medium as required after autoclaving to achieve a final concentration of $1\ \mu\text{g/ml}$.

Murine infection model. Mice used in this study were male BALB/c mice (Charles River) at 6 weeks of age, weighing approximately 20 to 25 g. Mice were infected intravenously with a dose of 1.25×10^6 spores of strain 1006PhL suspended in $100\ \mu\text{l}$ of sterile phosphate-buffered saline (PBS). Infected mice were monitored by weighing and visual scoring twice daily, and the mice were euthanized via CO_2

exposure when humane endpoints were reached (including but not limited to weight loss greater than 20% of starting body weight, or significant loss of grooming or mobility).

All intravenous infections were performed via retro-orbital injection unless otherwise noted, an approach developed based on previously published protocols (23). To perform retro-orbital injections, mice were anesthetized by exposure to inhaled isoflurane via the open-drop technique. Fungal inoculum suspended in PBS was then injected behind either the right or left eye, and the animal was visually monitored while recovering from anesthesia in room air.

As needed, mice were immunosuppressed 2 days prior to fungal infection. A single dose of 200 mg/kg cyclophosphamide in sterile PBS was delivered by intraperitoneal injection.

Strain isolation after *in vivo* passage. Mice were euthanized via CO₂ exposure at the humane endpoint, and up to five organs (brain, liver, spleen, kidney, and lung) were dissected. Whole organs were homogenized in 1 ml of sterile PBS through bead beating in a tube with two 5-mm steel beads (3 cycles of 1 min each). Organ homogenates were plated on YPD agar containing antibiotics (50 µg/ml ampicillin and 30 µg/ml chloramphenicol) for selective isolation of fungal colonies.

When hypoxic conditions were required, the GasPak EZ Container System was used (BD Diagnostics). YPD + antibiotic plates were placed in the GasPak Large Incubation Chamber, and three anaerobe sachets were added prior to sealing the chamber. Maintenance of hypoxic conditions (less than 1% O₂ and greater than 13% CO₂) was monitored using Dry Anaerobic Indicator Strips (BD).

If FK506 selection was required, 1 µg/ml FK506 was added to the YPD + antibiotic agar. Representative FK506-resistant (hyphal) and sensitive (yeast) colonies were picked for further analysis.

Fungal burden. Fungal burden was measured by plating organ homogenates (as described above) on YPD + antibiotic agar and counting colonies. This method does not produce a quantitative total for fungal burden in organs due to the breakup of hyphae into fragments during the bead beating step; however, the resulting counts allow for qualitative comparison between test groups of a given experiment and recovery of isolates for further analysis.

sRNA extraction and hybridization. Strains for sRNA extraction were grown on plates overlaid with sterile cellulose film (UV irradiated for 10 min per side) to allow for easier removal of hyphae. Small RNAs were extracted from hyphae using the mirVana miRNA Isolation kit (Ambion, Foster City, CA). Purified sRNA (3.5 µg) for each sample was separated by electrophoresis on 15% TRIS-urea gels.

When the 5S rRNA loading control was analyzed by ethidium bromide staining, sRNA gels were cut in half prior to transfer; the top half was stained with ethidium bromide and visualized under UV light, while the bottom half was transferred to Hybond N+ filters, and cross-linked by UV irradiation (2 pulses at 1.2×10^5 µJ per cm²) (17). When the 5S rRNA loading control was analyzed by radioactive probing instead, the entire gel was transferred to the membrane as described above.

Prehybridization of membranes was conducted using UltraHyb buffer (Ambion) at 65°C. *fkbA* antisense-specific and 5S rRNA riboprobes were prepared by *in vitro* transcription using the Maxiscript kit (Ambion); primers are listed in Table S2 in the supplemental material. Riboprobes were treated by alkaline hydrolysis as previously described (42) to generate an average final probe size of ~50 nucleotides. Hybridization was conducted overnight.

Statistics. Statistical significance of the Kaplan-Meier survival curves was determined using a log-rank test. One-way analyses of variance (ANOVAs) were used to determine significance when comparing rates of FK506 resistance, with Tukey's multiple-comparison test as a *post hoc* test where appropriate. All statistical analysis was performed using GraphPad Prism.

SUPPLEMENTAL MATERIAL

Supplemental material for this article may be found at <https://doi.org/10.1128/mBio.02579-19>.

FIG S1, TIF file, 0.1 MB.

FIG S2, TIF file, 0.3 MB.

TABLE S1, PDF file, 0.1 MB.

TABLE S2, PDF file, 0.1 MB.

ACKNOWLEDGMENTS

We thank Shelby Priest for critical reading of the manuscript. We also thank Jeffery Everitt, DVM of the Duke Research Animal Pathology Service for histopathologic analysis.

These studies were supported by NIH/NIAID R37 AI39115-21, R01 AI50113-15, P01 AI104533-05, and R01 AI112595-04. J.H. is co-director and fellow of the CIFAR program Fungal Threats & Opportunities.

REFERENCES

- Singh N, Aguado JM, Bonatti H, Forrest G, Gupta KL, Safdar N, John GT, Pursell KJ, Munoz P, Patel R, Fortun J, Martin-Davila P, Philippe B, Philit F, Tabah A, Terzi N, Chatelet V, Kusne S, Clark N, Blumberg E, Julia MB, Humar A, Houston S, Lass-Flörl C, Johnson L, Dubberke ER, Barron MA, Lortholary O. 2009. Zygomycosis in solid organ transplant recipients: a prospective, matched case-control study to assess risks for disease and outcome. *J Infect Dis* 200:1002–1011. <https://doi.org/10.1086/605445>.
- Roden MM, Zaoutis TE, Buchanan WL, Knudsen TA, Sarkisova TA,

- Schaufele RL, Sein M, Sein T, Chiou CC, Chu JH, Kontoyiannis DP, Walsh TJ. 2005. Epidemiology and outcome of zygomycosis: a review of 929 reported cases. *Clin Infect Dis* 41:634–653. <https://doi.org/10.1086/432579>.
3. Prakash H, Chakrabarti A. 2019. Global epidemiology of mucormycosis. *J Fungi (Basel)* 5:E26. <https://doi.org/10.3390/jof5010026>.
 4. Jeong W, Keighley C, Wolfe R, Lee W, Slavin MA, Kong D, Chen S. 2019. The epidemiology and clinical manifestations of mucormycosis: a systematic review and meta-analysis of case reports. *Clin Microbiol Infect* 25:26–34. <https://doi.org/10.1016/j.cmi.2018.07.011>.
 5. Kontoyiannis DP, Yang H, Song J, Kelkar SS, Yang X, Azie N, Harrington R, Fan A, Lee E, Spalding JR. 2016. Prevalence, clinical and economic burden of mucormycosis-related hospitalizations in the United States: a retrospective study. *BMC Infect Dis* 16:730. <https://doi.org/10.1186/s12879-016-2023-z>.
 6. Duffy J, Harris J, Gade L, Sehulster L, Newhouse E, O'Connell H, Noble-Wang J, Rao C, Balajee S, Chiller T. 2014. Mucormycosis outbreak associated with hospital linens. *Pediatr Infect Dis J* 33:472–476. <https://doi.org/10.1097/INF.0000000000000261>.
 7. Fanfair R, Benedict K, Bos J, Bennett SD, Lo Y-C, Adebajo T, Etienne K, Deak E, Derado G, Shieh W-J, Drew C, Zaki S, Sugerman D, Gade L, Thompson EH, Sutton DA, Engelthaler DM, Schupp JM, Brandt ME, Harris JR, Lockhart SR, Turabelidze G, Park BJ. 2012. Necrotizing cutaneous mucormycosis after a tornado in Joplin, Missouri, in 2011. *N Engl J Med* 367:2214–2225. <https://doi.org/10.1056/NEJMoa1204781>.
 8. Sundermann AJ, Clancy CJ, Pasculle WA, Liu G, Cumbie RB, Driscoll E, Ayres A, Donahue L, Pergam SA, Abbo L, Andes DR, Chandrasekar P, Galdys AL, Hanson KE, Marr KA, Mayer J, Mehta S, Morris MI, Perfect J, Revankar SG, Smith B, Swaminathan S, Thompson GR, Varghese M, Vazquez J, Whimbey E, Wingard JR, Nguyen HM. 2019. How clean is the linen at my hospital? The Mucorales on unclean linen discovery study of large United States transplant and cancer centers. *Clin Infect Dis* 68: 850–853. <https://doi.org/10.1093/cid/ciy669>.
 9. Kontoyiannis DP, Lewis RE. 2011. How I treat mucormycosis. *Blood* 118:1216–1224. <https://doi.org/10.1182/blood-2011-03-316430>.
 10. Marty FM, Ostrosky-Zeichner L, Cornely OA, Mullane KM, Perfect JR, Thompson GR, III, Alangaden GJ, Brown JM, Fredricks DN, Heinz WJ, Herbrecht R, Klimko N, Klyasova G, Maertens JA, Melinkeri SR, Oren I, Pappas PG, Racil Z, Rahav G, Santos R, Schwartz S, Vehreschild JJ, Young JH, Chetchotisakd P, Jaruratanasirikul S, Kanj SS, Engelhardt M, Kaufhold A, Ito M, Lee M, Sasse C, Maher RM, Zeiher B, Vehreschild M, VITAL and FungiScope Mucormycosis Investigators. 2016. Isavuconazole treatment for mucormycosis: a single-arm open-label trial and case-control analysis. *Lancet Infect Dis* 16:828–837. [https://doi.org/10.1016/S1473-3099\(16\)00071-2](https://doi.org/10.1016/S1473-3099(16)00071-2).
 11. Trieu TA, Navarro-Mendoza MI, Pérez-Arques C, Sanchis M, Capilla J, Navarro-Rodriguez P, Lopez-Fernandez L, Torres-Martínez S, Garre V, Ruiz-Vázquez RM, Nicolás FE. 2017. RNAi-based functional genomics identifies new virulence determinants in mucormycosis. *PLoS Pathog* 13:e1006150. <https://doi.org/10.1371/journal.ppat.1006150>.
 12. Rivaldi J, Carvalho AF, da Conceição LV, de Castro HF. 2017. Assessing the potential of fatty acids produced by filamentous fungi as feedstock for biodiesel production. *Prep Biochem Biotechnol* 47:970–976. <https://doi.org/10.1080/10826068.2017.1365246>.
 13. Trieu TA, Calo S, Nicolás FE, Vila A, Moxon S, Dalmay T, Torres-Martínez S, Garre V, Ruiz-Vázquez RM. 2015. A non-canonical RNA silencing pathway promotes mRNA degradation in basal fungi. *PLoS Genet* 11: e1005168. <https://doi.org/10.1371/journal.pgen.1005168>.
 14. Li CH, Cervantes M, Springer DJ, Boekhout T, Ruiz-Vázquez RM, Torres-Martínez SR, Heitman J, Lee SC. 2011. Sporangiospore size dimorphism is linked to virulence of *Mucor circinelloides*. *PLoS Pathog* 7:e1002086. <https://doi.org/10.1371/journal.ppat.1002086>.
 15. Silva F, Torres-Martínez S, Garre V. 2006. Distinct white collar-1 genes control specific light responses in *Mucor circinelloides*. *Mol Microbiol* 61:1023–1037. <https://doi.org/10.1111/j.1365-2958.2006.05291.x>.
 16. Garcia A, Adedoyin G, Heitman J, Lee SC. 2017. Construction of a recyclable genetic marker and serial gene deletions in the human pathogenic Mucorales *Mucor circinelloides*. *G3 (Bethesda)* 7:2047–2054. <https://doi.org/10.1534/g3.117.041095>.
 17. Calo S, Shertz-Wall C, Lee SC, Bastidas RJ, Nicolás FE, Granek JA, Mieczkowski P, Torres-Martínez S, Ruiz-Vázquez RM, Cardenas ME, Heitman J. 2014. Antifungal drug resistance evoked via RNAi-dependent epimutations. *Nature* 513:555–558. <https://doi.org/10.1038/nature13575>.
 18. Chang Z, Billmyre RB, Lee SC, Heitman J. 2019. Broad antifungal resistance mediated by RNAi-dependent epimutation in the basal human fungal pathogen *Mucor circinelloides*. *PLoS Genet* 15:e1007957. <https://doi.org/10.1371/journal.pgen.1007957>.
 19. Calo S, Nicolas FE, Lee SC, Vila A, Cervantes M, Torres-Martínez S, Ruiz-Vázquez RM, Cardenas ME, Heitman J. 2017. A non-canonical RNA degradation pathway suppresses RNAi-dependent epimutations in the human fungal pathogen *Mucor circinelloides*. *PLoS Genet* 13:e1006686. <https://doi.org/10.1371/journal.pgen.1006686>.
 20. Bastidas RJ, Shertz CA, Lee S, Heitman J, Cardenas ME. 2012. Rapamycin exerts antifungal activity *in vitro* and *in vivo* against *Mucor circinelloides* via FKBP12-dependent inhibition of Tor. *Eukaryot Cell* 11:270–281. <https://doi.org/10.1128/EC.05284-11>.
 21. Lee S, Li A, Calo S, Heitman J. 2013. Calcineurin plays key roles in the dimorphic transition and virulence of the human pathogenic zygomycete *Mucor circinelloides*. *PLoS Pathog* 9:e1003625. <https://doi.org/10.1371/journal.ppat.1003625>.
 22. Lee S, Li A, Calo S, Inoue M, Tonthat NK, Bain JM, Louw J, Shinohara ML, Erwig LP, Schumacher MA, Ko DC, Heitman J. 2015. Calcineurin orchestrates dimorphic transitions, antifungal drug responses and host-pathogen interactions of the pathogenic mucoralean fungus *Mucor circinelloides*. *Mol Microbiol* 97:844–865. <https://doi.org/10.1111/mmi.13071>.
 23. Yardeni T, Eckhaus M, Morris HD, Huizing M, Hoogstraten-Miller S. 2011. Retro-orbital injections in mice. *Lab Anim (NY)* 40:155–160. <https://doi.org/10.1038/aban0511-155>.
 24. Jacobsen ID. 2019. Animal models to study mucormycosis. *J Fungi (Basel)* 5:E27. <https://doi.org/10.3390/jof5020027>.
 25. Steel CD, Stephens AL, Hahto SM, Singletary SJ, Ciavarrá RP. 2008. Comparison of the lateral tail vein and the retro-orbital venous sinus as routes of intravenous drug delivery in a transgenic mouse model. *Lab Anim (NY)* 37:26. <https://doi.org/10.1038/aban0108-26>.
 26. Price JE, Barth RF, Johnson CW, Staubus AE. 1984. Injection of cells and monoclonal antibodies into mice: comparison of tail vein and retro-orbital routes. *Proc Soc Exp Biol Med* 177:347–353. <https://doi.org/10.3181/00379727-177-41955>.
 27. Bartnicki-Garcia S, Nickerson WJ. 1962. Induction of yeast-like development in *Mucor* by carbon dioxide. *J Bacteriol* 84:829–840.
 28. Asner SA, Giulieri S, Diezi M, Marchetti O, Sanglard D. 2015. Acquired multidrug antifungal resistance in *Candida lusitanae* during therapy. *Antimicrob Agents Chemother* 59:7715–7722. <https://doi.org/10.1128/AAC.02204-15>.
 29. Dannaoui E. 2017. Antifungal resistance in Mucorales. *Int J Antimicrob Agents* 50:617–621. <https://doi.org/10.1016/j.ijantimicag.2017.08.010>.
 30. Young LY, Hull CM, Heitman J. 2003. Disruption of ergosterol biosynthesis confers resistance to amphotericin B in *Candida lusitanae*. *Antimicrob Agents Chemother* 47:2717–2724. <https://doi.org/10.1128/aac.47.9.2717-2724.2003>.
 31. Luna-Tapia A, Willems HME, Parker JE, Tournu H, Barker KS, Nishimoto AT, Rogers DP, Kelly SL, Peters BM, Palmer GE. 2018. Loss of Upc2p-inducible *ERG3* transcription is sufficient to confer niche-specific azole resistance without compromising *Candida albicans* pathogenicity. *mBio* 9:e00225-18. <https://doi.org/10.1128/mBio.00225-18>.
 32. Kelly SL, Lamb DC, Kelly DE, Manning NJ, Loeffler J, Hebart H, Schumacher U, Einsele H. 1997. Resistance to fluconazole and cross-resistance to amphotericin B in *Candida albicans* from AIDS patients caused by defective sterol delta5,6-desaturation. *FEBS Lett* 400:80–82. [https://doi.org/10.1016/s0014-5793\(96\)01360-9](https://doi.org/10.1016/s0014-5793(96)01360-9).
 33. Kelly SL, Lamb DC, Kelly DE, Loeffler J, Einsele H. 1996. Resistance to fluconazole and amphotericin in *Candida albicans* from AIDS patients. *Lancet* 348:1523–1524. [https://doi.org/10.1016/S0140-6736\(05\)65949-1](https://doi.org/10.1016/S0140-6736(05)65949-1).
 34. Nolte FS, Parkinson T, Falconer DJ, Dix S, Williams J, Gilmore C, Geller R, Wingard JR. 1997. Isolation and characterization of fluconazole- and amphotericin B-resistant *Candida albicans* from blood of two patients with leukemia. *Antimicrob Agents Chemother* 41:196–199. <https://doi.org/10.1128/AAC.41.1.196>.
 35. Robbins N, Collins C, Morhayim J, Cowen LE. 2010. Metabolic control of antifungal drug resistance. *Fungal Genet Biol* 47:81–93. <https://doi.org/10.1016/j.fgb.2009.07.004>.
 36. Prakash H, Ghosh A, Rudramurthy S, Paul R, Gupta S, Negi V, Chakrabarti A. 2016. The environmental source of emerging *Apophysomyces variabilis* infection in India. *Med Mycol* 54:567–575. <https://doi.org/10.1093/mmy/myw014>.
 37. Kino T, Hatanaka H, Hashimoto M, Nishiyama M, Goto T, Okuhara M, Kohsaka M, Aoki H, Imanaka H. 1987. FK-506, a novel immunosuppressant isolated from a *Streptomyces*. I. Fermentation, isolation, and

- physico-chemical and biological characteristics. *J Antibiot (Tokyo)* 40: 1249–1255. <https://doi.org/10.7164/antibiotics.40.1249>.
38. Sehgal SN, Baker H, Vézina C. 1975. Rapamycin (AY-22,989), a new antifungal antibiotic. II. Fermentation, isolation and characterization. *J Antibiot (Tokyo)* 28:727–732. <https://doi.org/10.7164/antibiotics.28.727>.
39. Snyder AB, Churey JJ, Worobo RW. 2016. Characterization and control of *Mucor circinelloides* spoilage in yogurt. *Int J Food Microbiol* 228:14–21. <https://doi.org/10.1016/j.ijfoodmicro.2016.04.008>.
40. Lee S, Billmyre BR, Li A, Carson S, Sykes SM, Huh E, Mieczkowski P, Ko DC, Cuomo CA, Heitman J. 2014. Analysis of a food-borne fungal pathogen outbreak: virulence and genome of a *Mucor circinelloides* isolate from yogurt. *mBio* 5:e01390-14. <https://doi.org/10.1128/mBio.01390-14>.
41. Mueller KD, Zhang H, Serrano CR, Billmyre BR, Huh E, Wiemann P, Keller NP, Wang Y, Heitman J, Lee S. 2019. Gastrointestinal microbiota alteration induced by *Mucor circinelloides* in a murine model. *J Microbiol* 57:509–520. <https://doi.org/10.1007/s12275-019-8682-x>.
42. Nicolas FE, Torres-Martinez S, Ruiz-Vazquez RM. 2003. Two classes of small antisense RNAs in fungal RNA silencing triggered by non-integrative transgenes. *EMBO J* 22:3983–3991. <https://doi.org/10.1093/emboj/cdg384>.